P2.15 LONG RANGE LIGHTNING NOWCASTING APPLICATIONS FOR TROPICAL CYCLONES

Nicholas W.S. Demetriades and Ronald L. Holle
Vaisala, Inc., Tucson, Arizona

1. INTRODUCTION

The outer limit of land-based CG flash detection networks is set at 625 km from sensors in the U.S. National Lightning Detection Network (NLDN) and the Canadian Lightning Detection Network (CLDN). This distance is determined by characteristics of the radiation emitted by the ground waves from CG flashes (Section 2). While 625 km is beyond the range of coastal meteorological radars, it is not especially far from land for monitoring rapid changes in tropical cyclone structure and intensity. The primary sources for monitoring hurricanes beyond this 625-km range are (1) infrared and visible satellite imagery provided by geostationary satellites, (2) microwave and space-based radar imagery provided by polar orbiting satellites and (3) air reconnaissance data provided by National Oceanic and Atmospheric Administration (NOAA) and U.S. Air Force hurricane hunters. Geostationary satellite imagery is the only one of these datasets that provides continuous monitoring of tropical cyclones. Unfortunately, such imagery often does not provide all the necessary detailed structural information in eyewalls and outer rainbands that meteorologists need for nowcasting/forecasting tropical cyclones.

Vaisala is currently operating a VLF long-range lightning detection network (LLDN) over the northern Atlantic and Pacific Oceans that detects flashes thousands of kilometers from sensors in North America, Europe and Asia. LLDN data may provide meteorologists a valuable, continuous data set that reveals the stronger convective structures within tropical cyclones over a large portion of the Atlantic and Eastern Pacific tropical cyclone basins.

Lightning within eyewalls of some hurricanes near the coast have been studied with respect to eyewall contraction or secondary eyewall replacement (Molinari et al., 1999). Demetriades and Holle (2005) expanded this prior research to strong hurricanes over much larger areas than previously possible. This paper will describe continuing work within Vaisala to examine the structure of eyewall lightning outbreaks, including LLDN data from Hurricanes Katrina and Rita.

In addition, detection of flashes in outer rainbands of tropical cyclones may provide forecasters with a valuable diagnostic tool. For many areas that do not experience the inner core of the hurricane, intense outer rainbands contain the most hazardous weather. In weaker tropical cyclones, such as tropical depressions and storms, intense rainbands often contain the highest wind speeds and heaviest rainfall. Outer rainband lightning will also be discussed in this paper.

*Corresponding author address: Nicholas W.S. Demetriades, Vaisala, Inc., Tucson, AZ 85706; email; nick.demetriades@vaisala.com

2. LONG-RANGE LIGHTNING DETECTION NETWORK (LLDN)

NLDN and CLDN wideband sensors operate in the frequency range from about 0.5 to 400 kHz where return strokes in CG flashes radiate most strongly. The peak radiation from CG flashes comes near 10 kHz in the middle of the very low frequency (VLF) band of 3-30 kHz. Signals in the VLF band are trapped in the earth-ionosphere waveguide and suffer relatively less severe attenuation than higher frequency signals. Low frequency (LF) and VLF ground wave signals from CGs are attenuated strongly, and are almost imperceptible after a propagation distance of 500 to 1000 km. However, VLF signals may be detected several thousand kilometers away after one or more reflections off the ground and the ionosphere. Detection is best when both a lightning source and a sensor are on the night side of the earth, because of better ionospheric propagation conditions at night. The NLDN can easily detect and process signals from lightning at long distances because the standard sensors in the network detect across a broad band that includes all of the VLF.

Standard NLDN sensors have been part of an ongoing experimental long-range detection network consisting of the combination of the CLDN, the Japanese Lightning Detection Network, the Meteo-France network, and the BLIDS, Benelux, and Central European networks operated by Siemens in Germany. This combination of networks detects CG flashes in sufficient numbers and with sufficient accuracy to identify small thunderstorm areas. The network detects CGs to varying degrees over the northern Atlantic and Pacific oceans, and also over some areas of Asia and Latin America not covered by local ground-based lightning detection networks.

3. TROPICAL CYCLONE LIGHTNING NOWCASTING APPLICATIONS

The LLDN continuously monitors lightning activity in tropical cyclones over a large portion of the Atlantic and Eastern Pacific tropical cyclone basins. Lightning activity in tropical cyclones has been examined in several studies (Molinari et al., 1994; 1999; Lyons and Keen, 1994; Black and Hallett, 1999; Cecil et al., 2002; Samsury and Orville, 1994; Sugita and Matsui, 2004; Demetriades and Holle, 2005). Most studies

used NLDN data, and one used lightning detected by the Lightning Imaging Sensor (LIS) located onboard the Tropical Rainfall Measuring Mission (TRMM) satellite. Past analyses of lightning activity in tropical cyclones from the NLDN were limited to regions within ~400 km of the U.S. coastline. Analysis of lightning activity in tropical cyclones from LIS were limited to TRMM overpasses that occurred no more than twice a day for 90 seconds at a time.

Tropical depressions and tropical storms are generally more prolific lightning producers than hurricanes. Lightning activity in these systems does not show a preferential spatial pattern. New observations of CG lightning activity within numerous tropical cyclones over the Atlantic and Eastern Pacific Oceans away from land have reinforced many of the findings of Molinari et al. (1999).

Figure 1 shows the lightning activity produced by Tropical Storm Katrina between 1415 and 1445 UTC 24 August 2005. Katrina was located just northeast of Cuba at this time and was a minimal tropical storm with sustained winds of 40 miles per hour (64 kilometers per hour). Katrina was producing a large amount of lighting during this 30-minute time period in a number of convective clusters that covered most of the cloud mass of the storm.

Lightning does show preferential spatial patterns in hurricanes. The eyewall (or inner core) usually contains a weak maximum in lightning flash density. There is a well-defined minimum in flash density extending 80 to 100 km outside the eyewall maximum (Molinari et al., 1999). This is due to the stratiform rain processes that generally dominate most of the region of the central dense overcast. The outer rain bands typically contain a strong maximum in flash density. Figure 2 shows the lightning activity within Katrina between 1845 and 1915 UTC 28 August 2005

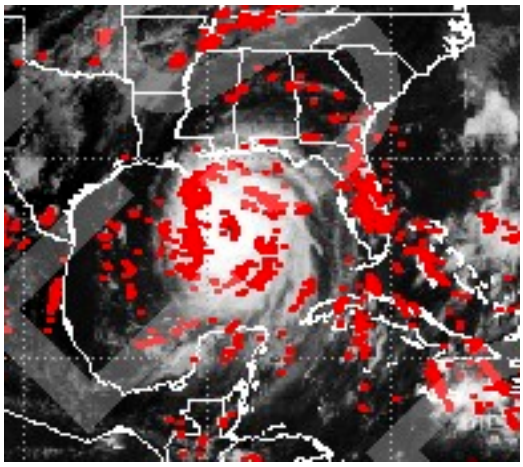

Figure 2. Same as Figure 1, except for Hurricane Katrina between 1845 and 1915 UTC 28 August 2005. Infrared satellite image from 1915 UTC.

as it had strengthened to a category five hurricane on the Saffir-Simpson Scale. The lightning activity in Hurricane Katrina shows a large eyewall lightning outbreak, very little lightning in the central dense overcast and a tremendous amount of lightning in outer rainbands surrounding most of the storm. There is a much more defined pattern to the lightning activity in Hurricane Katrina (Fig. 2) when compared to its tropical storm stage (Fig. 1). The lightning pattern in category five Hurricane Rita from 0615 to 0645 UTC 22 September 2005 shows a similar large eyewall lightning outbreak and minimal lightning activity in the central dense overcast, but very little lightning in outer rainbands (Fig. 3). A comparison of lightning activity in category five Hurricanes Katrina and Rita shows an

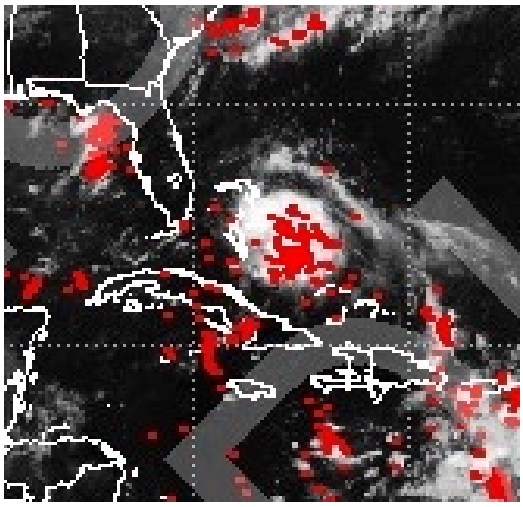

Figure 1. CG lightning (red symbols) detected within Tropical Storm Katrina between 1415 and 1445 UTC 24 August 2005. Infrared satellite image from 1445 UTC.

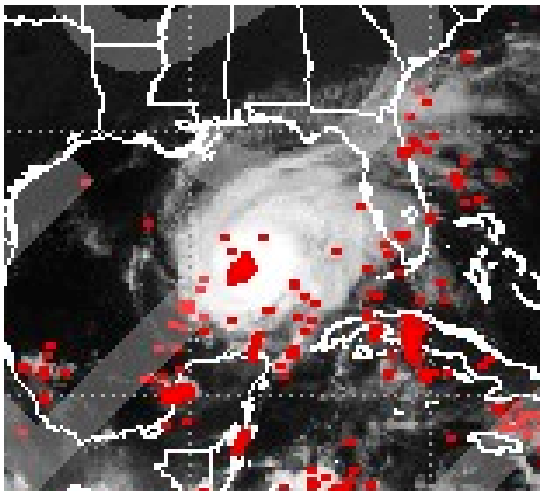

Figure 3. Same as Figure 1, except for Hurricane Rita between 0615 and 0645 UTC 22 September 2005. Infrared satellite image from 0645 UTC.

organized pattern to the lightning activity consisting of eyewall lightning and minimal lightning in the central dense overcast of each storm (Figs. 2 and 3). However, these examples also demonstrate the variability in the structure and existence of outer rainband lightning.

4. OUTER RAINBAND LIGHTNING

Lightning activity can help identify the most intense outer rainbands in a tropical cyclone. These rainbands often contain flooding rains and strong, gusty winds. Lightning can also show the evolution of growth and dissipation of outer rainbands as they rotate around the periphery of the storm. For many areas that do not experience the inner core of the hurricane, intense outer rainbands contain the most hazardous weather. Figure 4 shows CG lightning detected within Hurricane Ivan between 1345 and 1415 UTC 15 September 2004 as it moved toward the U.S. coastline in the Gulf of Mexico. Lightning activity clearly delineates an intense outer rainband located on the east side of Ivan. Some other strong rainbands are shown by lightning data toward the south and southeast of the center of Ivan.

Hurricane Frances was a powerful category 3 hurricane on the Saffir-Simpson scale during the time period shown in Figure 5. Usually, high rates of lightning activity occur in one or two dominant rainbands located on one side of the hurricane. Frances was somewhat unique during this time as lightning activity indicated intense outer rainbands surrounding most of the storm.

Figure 6 shows the evolution of an outer rainband as it rotates counterclockwise around the center of Hurricane Fabian on 5 September 2003. Between 1253 and 1553 UTC, lightning activity indicated that the most intense outer rainband rotated from a position located toward the east of the center of Fabian (yellow) to north of Fabian (red).

In weaker tropical cyclones, such as tropical depressions and storms, intense rainbands often contain the highest wind speeds and heaviest rainfall. In order to properly issue tropical depression and storm advisories and warnings, it is critical to be able to identify the location and evolution of these features. An example of this is shown in Figure 7, where intense outer rainbands were identified by high rates of lightning activity located toward the southeast of Tropical Storm Kyle.

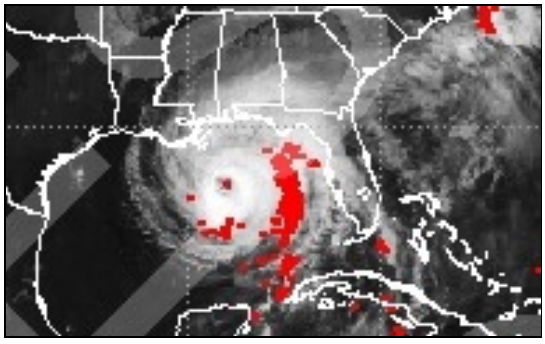

Figure 4. Same as Figure 1, except for Hurricane Ivan between 1345 and 1415 UTC 15 September 2004. Infrared satellite image from 1415 UTC.

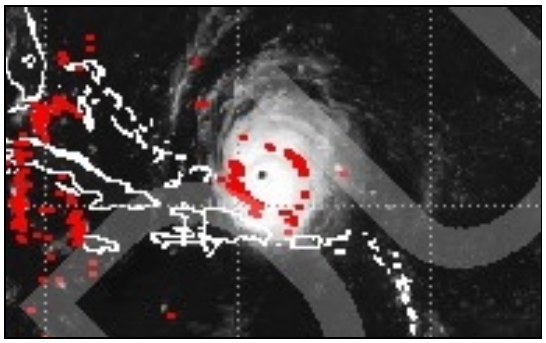

Figure 5. Same as Figure 1, except for Hurricane Frances between 0945 and 1015 UTC 1 September 2004. Infrared satellite image from 1015 UTC.

5. EYEWALL LIGHTNING OUTBREAKS

5.1 Eyewall lightning patterns

The LLDN has detected eyewall lightning outbreaks in many hurricanes from both the Atlantic and Eastern Pacific tropical cyclone basins during the past several years. The larger eyewall lightning outbreaks tend to occur on relatively small time and space scales. Lightning bursts in the eyewalls of hurricanes sometimes rotate counterclockwise around the center of circulation for some distance before they

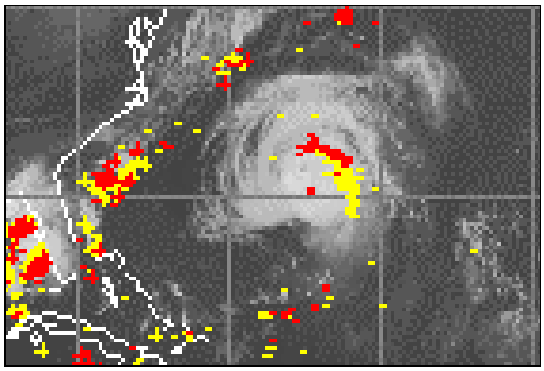

Figure 6. Long range lightning data and infrared satellite image on 5 September 2003. Lightning is for 3 hours from 1253 to 1553 UTC. Yellow dots are flashes detected during the first two hours from 1253 to 1453 UTC, and red are from the latest hour from 1453 to 1553. Infrared satellite image is from 1553 UTC.

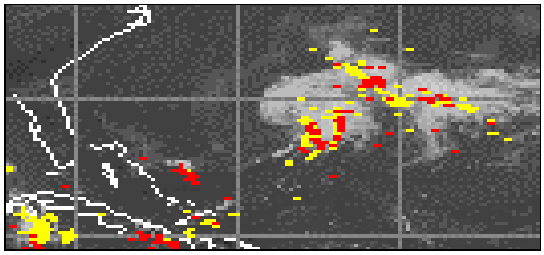

Figure 7. Same as Figure 6, except for Tropical Storm Kyle between 1453 and 1753 UTC 2 October 2002. Infrared satellite image is from 1753 UTC.

dissipate. However, eyewall lightning outbreaks that were studied in several hurricanes since 2002 show that these outbreaks tend to preferentially occur on one side of the hurricane track. Several hours may separate consecutive bursts of eyewall lightning or these bursts may occur continually for 24-48 hours. Figure 8 shows lightning detected along the track of Hurricane Frances between 0000 UTC 3 September and 0000 UTC 4 September 2004. The track of Frances during this 24-hour period is shown by the yellow and red line. Three eyewall lightning outbreaks can be identified as Frances moved toward the northwest. All three of the outbreaks occurred on the northeast side of the storm track. The first outbreak is shown in green, the second outbreak in orange and the final outbreak on this day in red.

Hurricane Katrina produced large eyewall lightning outbreaks throughout a significant portion of its lifetime. Figure 9 shows one of these outbreaks as the storm was undergoing significant intensification from a category one to a category five hurricane on the Saffir-Simpson Scale. Lightning flash densities between 1637:30 and 1652:30 UTC 26 August 2005 are shown in colors ranging from light blue to pink. Light blue (pink) represents one flash (greater than 10 flashes) per 16 square kilometer area for the time interval shown. The track of Katrina as it moved through southern Florida and into the southeastern part of the Gulf of Mexico is shown by the white line. NHC estimated center position of Katrina (red dot) at 1630 UTC 26 August shows that this outbreak occurred in the southeastern portion of the eyewall. Although the lightning flashes are confined to a specific quadrant within the eyewall of Katrina, notice that it is a different quadrant from that found in Hurricane Frances (Fig. 8). A comparison with a radar base reflectivity image from the Key West WSR-88D at 1645 UTC shows that the high eyewall lightning rates were associated with base reflectivities greater than 50 dBZ (Fig. 10). Vaisala is currently exploring relationships between eyewall lightning outbreaks and radar reflectivity signatures.

Hurricane Rita produced some impressive eyewall lightning signatures as it became a category five hurricane on 21 September 2005. At times, Rita produced significant eyewall lightning that surrounded almost the entire eyewall. Figure 11 shows an example of this between 1430 and 1500 UTC 21 September. Eyewall lightning outlines the northeast, northwest and southwest portions of the eyewall of Rita during this time period. In this case, lightning data could have been used to show that strong convection, and by implication large latent heat release, was simultaneously occurring throughout approximately 75 percent of the eyewall.

Eyewall lightning tends to occur when the inner core of the hurricane is undergoing a change in structure and intensity. Lightning helps to identify intense convective cores with larger updraft speeds embedded in the eyewalls of hurricanes. These lightning outbreaks may be strongly, and perhaps uniquely, associated with tall precipitation features, often called hot towers, that form in hurricane eyewalls. In favorable environments for hurricane intensification, these tall precipitation features are often associated with rapid intensification of hurricanes. Vaisala continues to collaborate with the tropical meteorology community in order to determine how often eyewall lightning outbreaks are associated with tall precipitation features within hurricane eyewalls.

5.2 Hurricane Rita

Rita developed north of the Dominican Republic on 18 September 2005. Rita then propagated to the west and attained hurricane status at 15 UTC 20 September, as it passed just south of the Florida Keys. Twelve hours later, Rita was already classified as a category five hurricane on the Saffir-Simpson Scale with sustained wind speeds of 175 miles per hour (282 kilometers per hour) and a minumum central pressure of 897 millibars (mb). This is the fourth lowest pressure ever recorded for a hurricane in the Atlantic Basin. Rita eventually turned to the northwest and made landfall as a category three hurricane just east of Sabine Pass, Texas at 0730 UTC 24 September.

A time series of minimum central pressure and eyewall lightning rates from Hurricane Rita shows bursts of eyewall lightning during rapid intensification (Figure 12). Minimum central pressure for the storm was obtained from National Hurricane Center (NHC) Forecast Discussions. Eyewall lightning rates were defined as the number of lightning flashes detected by the Vaisala LLDN within 100 km of the center of Rita (as reported by NHC) per three-hour interval.

The first large eyewall lightning outbreak started at 15 UTC 19 September as three-hour eyewall lightning rates rapidly increased from values well under 100 to values over 400 (Fig. 12). These large lightning rates continued until 06 UTC 20 September and peaked with the largest eyewall lightning rate throughout the history of the storm. This peak eyewall lightning rate contained 1340 flashes at 00 UTC 20 September. Rita started to rapidly intensify from the time of the 1340 eyewall lightning peak and attained hurricane status at 15 UTC 20 September. Shortly after Rita attained hurricane status, another very large eyewall lightning outbreak occurred with a peak three-hour

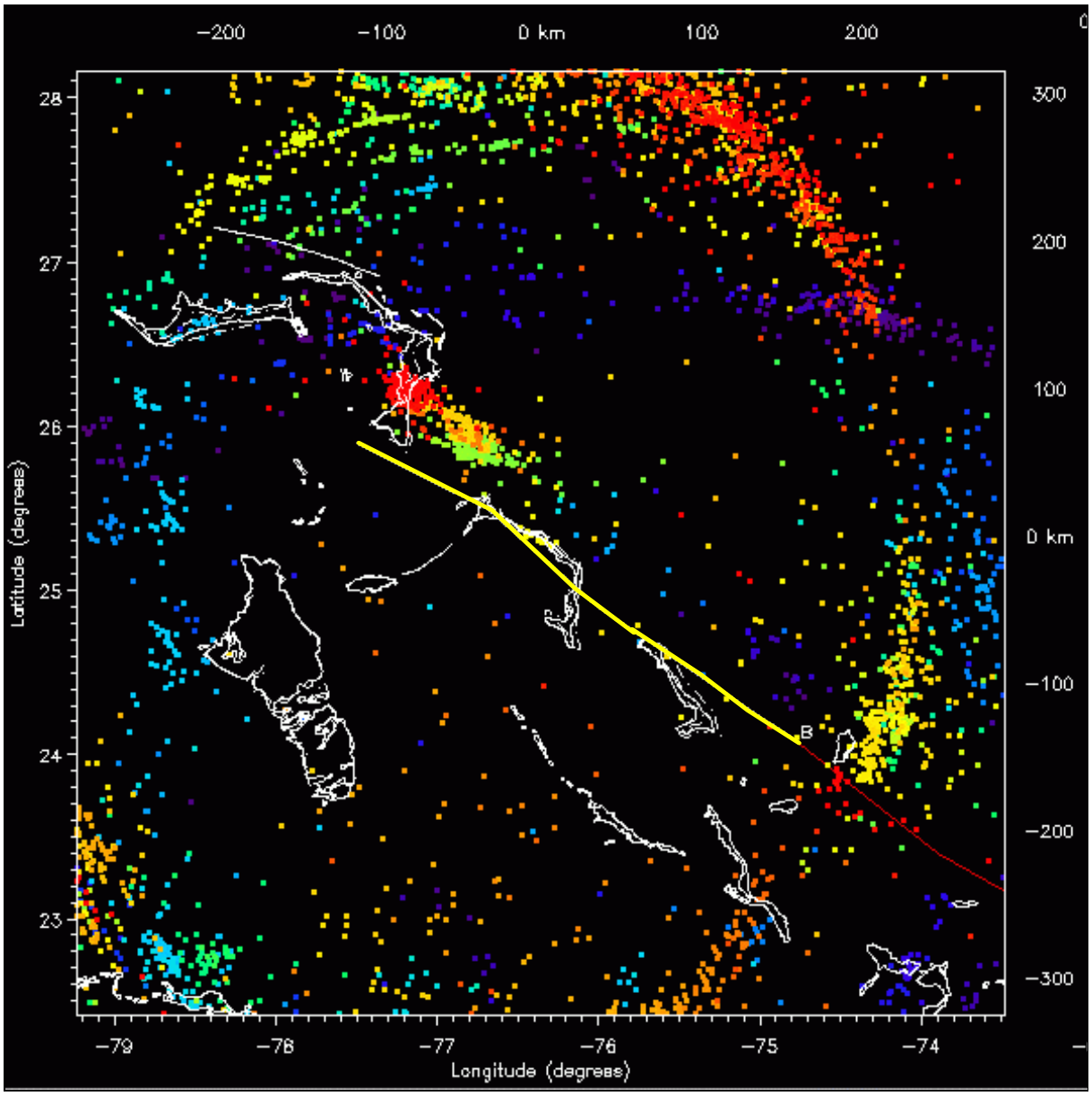

Figure 8. CG lightning detected by the LLDN in Hurricane Frances between 0000 UTC 3 September and 0000 UTC 4 September 2004. The track of the center of Frances during this 24-hour period is shown by the yellow line. Three bursts of eyewall lightning are along the right side of the track of Frances as the storm moved toward the northwest (upper left). The first burst of eyewall lightning is in green, the second burst is in orange, and the third burst is in red.

rate of 997 flashes at 21 UTC 20 September. This second, major eyewall lightning outbreak occurred as the storm began to intensify at a higher rate with the central pressure dropping from 973 to 956 mb (hPa) between 21 UTC 20 September and 09 UTC 21 September. A third large eyewall lightning outbreak occurred at 15 UTC 21 September when 820 flashes were detected. This outbreak was coincident with the beginning of the most rapid intensification of the storm as the pressure dropped an average of 3.9 mb (hPa) per hour from 15 UTC 21 September to 03 UTC 22 September. At the end of this rapid intensification, Rita's minimum central pressure was 897 mb (hPa). As Rita's intensification ceased, eyewall lightning rates increased one more time to values between 300 and 500 from 00 to 06 UTC 22 September. This final large increase in lightning rates may be the first signs of secondary eyewall formation as the 09 UTC 22 September NHC Forecast Discussion mentioned that a secondary eyewall was forming in Rita. This would

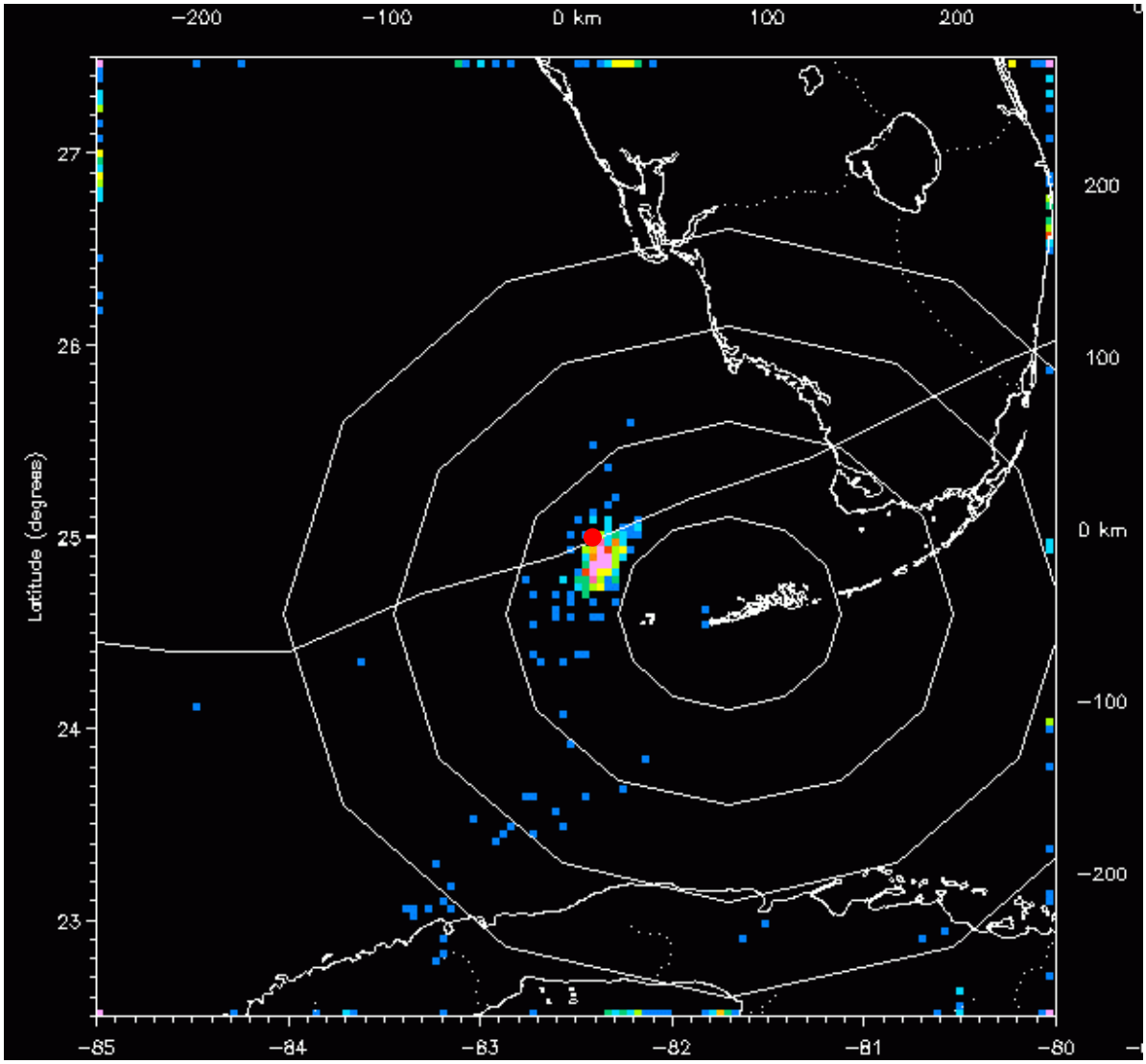

Figure 9. Lightning flash densities detected in Hurricane Katrina between 1637:30 and 1652:30 UTC 26 August 2005. Densities are shown in colors ranging from light blue to pink. Light blue (pink) represents one flash (greater than 10 flashes) per 16 square kilometer area for the time interval shown. The track of Katrina as it moved through southern Florida and into the southeastern part of the Gulf of Mexico is shown by the white line. The National Hurricane Center estimated center position of Katrina (red dot) at 1630 UTC 26 August shows that this outbreak occurred in the southeastern portion of the eyewall.

be consistent with some of the findings of Molinari et al. (1999) and Demetriades and Holle (2005).

5.3 Lack of eyewall lightning – Hurricane Isabel

Demetriades and Holle (2005) found evidence to support the Molinari et al. (1999) hypothesis that a hurricane that has been fairly steady in intensity will remain fairly steady in intensity when little or no eyewall lightning is present. Therefore, a lack of eyewall lightning or very low eyewall lightning rates may be another valuable tool that can aid forecasters in hurricane nowcasting.

Hurricane Isabel had a long period without eyewall lightning while it was very strong. The storm developed west of Africa and moved WNW to the NE of the Caribbean islands. Isabel made landfall on the North Carolina coast on 18 September as a category 2 hurricane with sustained winds of 104 miles per hour (167 kilometers per hour). On 11 September Isabel intensified to category 5 status on the Saffir-Simpson Scale and reached a maximum intensity of 167 miles per hour (269 kilometers per hour). Isabel had already reached its maximum intensity before reaching the 10% CG lightning detection efficiency area off the coast of the U.S. Figure 13 shows the

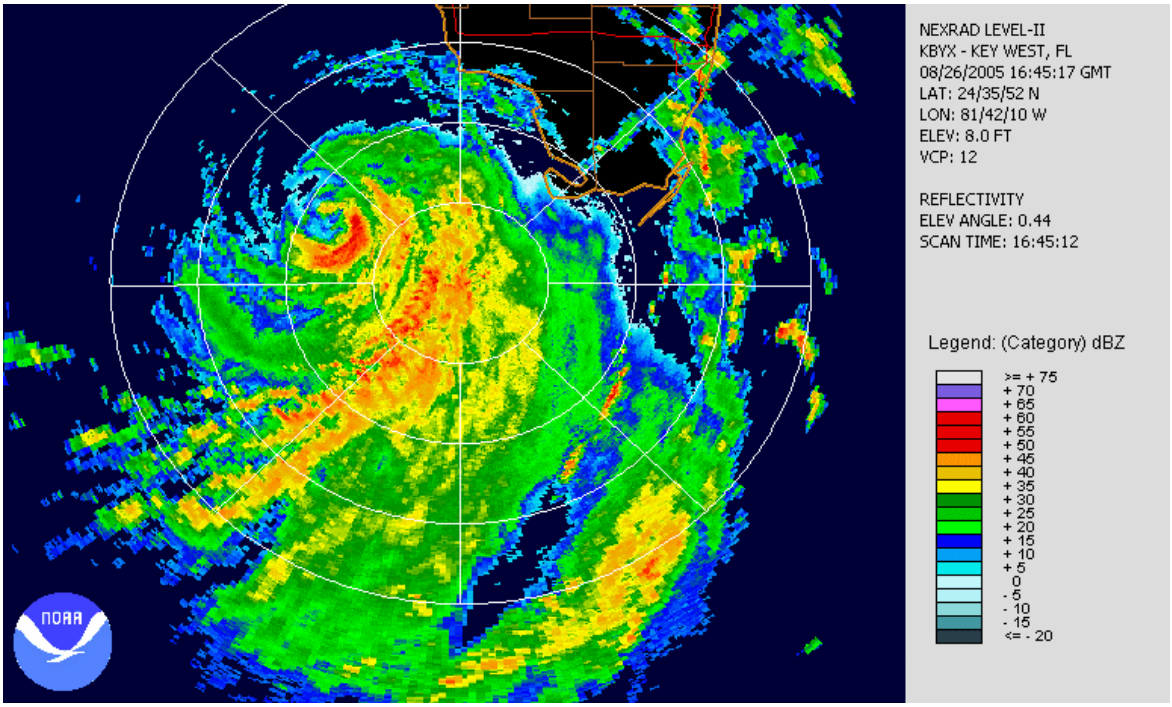

Figure 10. Key West WSR-88D base reflectivity image from 1645 UTC 26 August 2005. Reflectivity values are shown on the lower right. The highest reflectivities are located in the southeastern portion of the eyewall.

eyewall flash rate superimposed upon observations of central pressure from Hurricane Isabel during the period of analysis. One eyewall lightning flash was detected near 1200 UTC 14 September as the storm was about to undergo a fairly rapid weakening stage. Another eyewall lightning outbreak occurred between 0900 UTC 15 September and 0300 UTC 16 September. There were only a total of 5 CG flashes detected, however they occurred during a time period of concentric eyewall formation. The NHC discussion at 0900 UTC 15 September stated "The aircraft has also reported well-defined concentric wind maxima." Isabel maintained a fairly steady central pressure between 1200 UTC 16 September and 0900 UTC 18 September. During this time period, no eyewall lightning was detected in this storm. This is in agreement with the Molinari et al. (1999) hypothesis that hurricanes undergoing little change in intensity will not exhibit eyewall flashes. A final outbreak of eyewall lightning occurred between 1500 and 1800 UTC 18 September. This outbreak was probably initially caused by concentric eyewall formation before being influenced by landfall. The NHC discussion at 0900 UTC 18 September stated "WSR-88D radar data from Morehead City shows what looks like a classic concentric eyewall formation…with a poorly-defined ring of convection near the center and a stronger ring 40-50 nm out."

6. CONCLUSIONS

Real-time lightning data over a large portion of the northern Atlantic and Eastern Pacific tropical cyclone basins is now being provided by Vaisala's LLDN. The data should allow forecasters to continuously monitor the evolution of strong convective structures in the eyewalls of tropical cyclones. In Hurricane Rita, strong convective structures producing large amounts of eyewall lightning were mostly associated with rapid storm intensification. In addition, lightning should help identify and track the most intense outer rainbands. For areas outside the inner core, and in weaker tropical cyclones, intense rainbands often contain the highest wind speeds and heaviest rainfall. In order to issue the appropriate advisories and warnings, forecasters need to be able to follow the evolution of strong convective features in the eyewall and outer rainbands of tropical cyclones. Vaisala LLDN data may provide the best opportunity to follow these important features over data-sparse oceanic areas.

7. REFERENCES

Black, R.A., and J. Hallett, 1999: Electrification of the hurricane. *J. Atmos. Sci.,* **56**, 2004-2028.

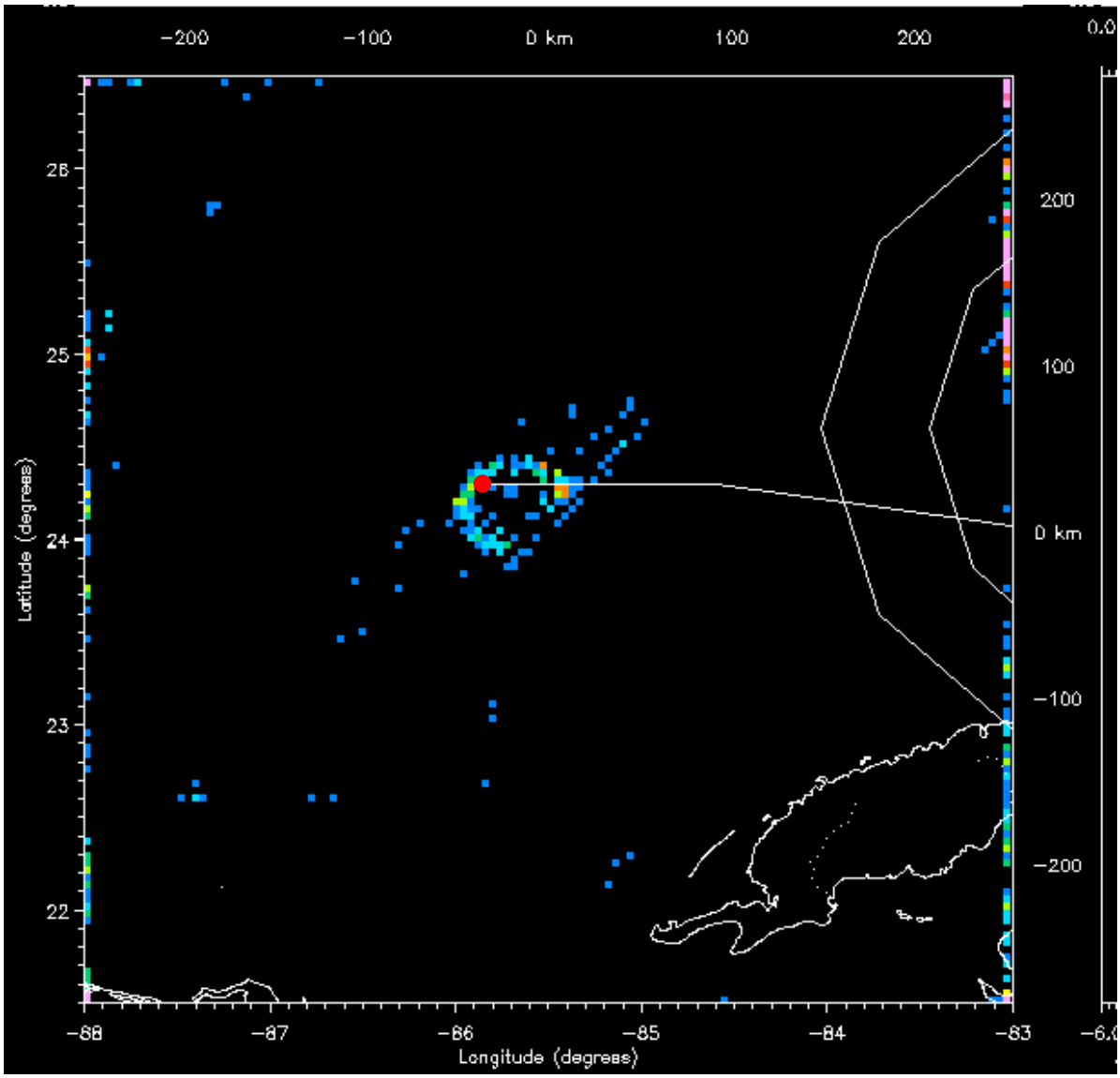

Figure 11. Same as Figure 9, except for Hurricane Rita between 1430 and 1500 UTC 21 September 2005. Red dot represents the National Hurricane Center estimated center position of Rita at 1500 UTC 21 September 2005.

Cecil, D.J., E.J. Zipser and S.W. Nesbitt, 2002: Reflectivity, ice scattering, and lightning characteristics of hurricane eyewalls and rainbands. Part I: Quantitative description. *Mon. Wea. Rev.,* **130**, 769–784.

Demetriades, N.W.S., and R.L. Holle, 2005: Long-range lightning applications for hurricane intensity and precipitation nowcasting. *Preprints, Conf. on Meteor. Appl. of Lightning Data,* San Diego, Jan. 9-13, Amer. Meteor. Soc., 9 pp.

Lyons, W.A., and C.S. Keen, 1994: Observations of lightning in convective supercells within tropical storms and hurricanes. *Mon. Wea. Rev.,* **122,** 1897-1916.

Molinari, J., P. Moore, and V. Idone, 1999: Convective structure of hurricanes as revealed by lightning locations. *Mon. Wea. Rev.*, **127**, 520-534.

—, P.K. Moore, V.P. Idone, R.W. Henderson, and A.B. Saljoughy, 1994: Cloud-to-ground lightning in Hurricane Andrew. *J. Geophys. Res.*, **99**, 16665-16676.

Samsury, C.E., and R.E. Orville, 1994: Cloud-to-ground lightning in tropical cyclones: A study of Hurricanes Hugo (1989) and Jerry (1989). *Mon. Wea. Rev.,* **122**, 1887-1896.

Sugita, A., and M. Matsui, 2004: Lightning in typhoons observed by JLDN. *Proceedings, 18th Intl. Lightning Detection Conf.*, June 7-9, Helsinki, Finland, Vaisala, 4 pp.

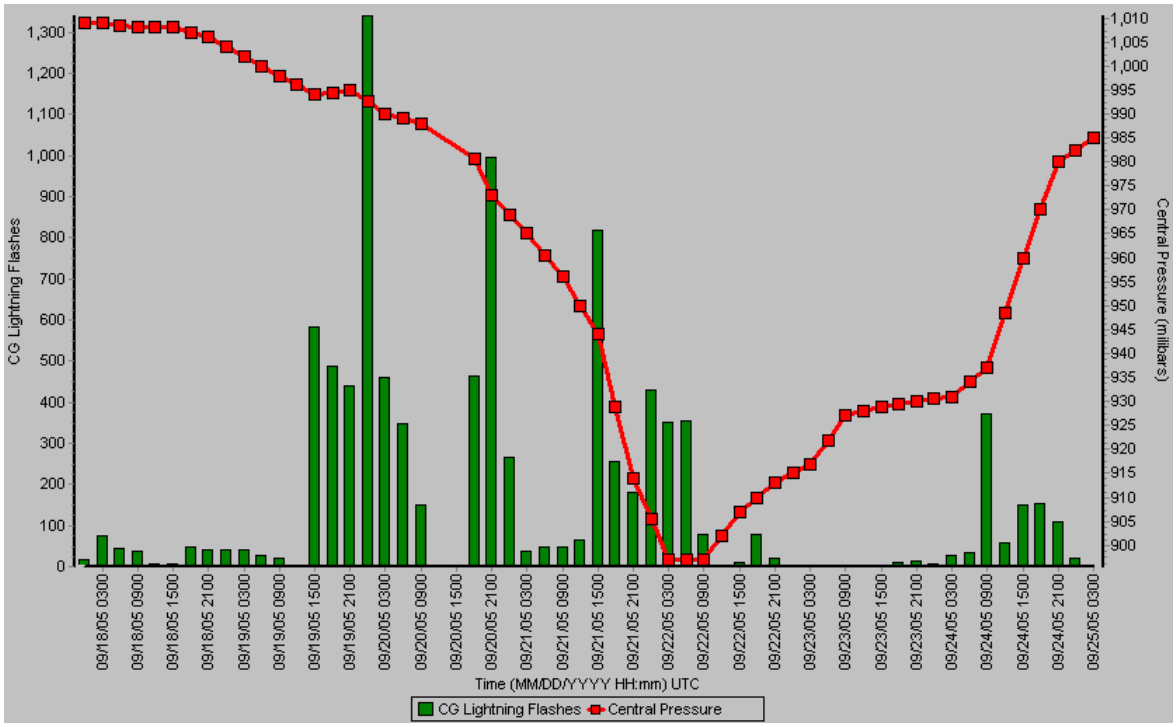

Figure 12. Three-hour CG lightning rates detected within 100 km of Hurricane Rita's center superimposed on Rita's central pressure. CG lightning rates are indicated by green bars with values located on the left y-axis and central pressure is indicated by the red line with values located on the right y-axis.

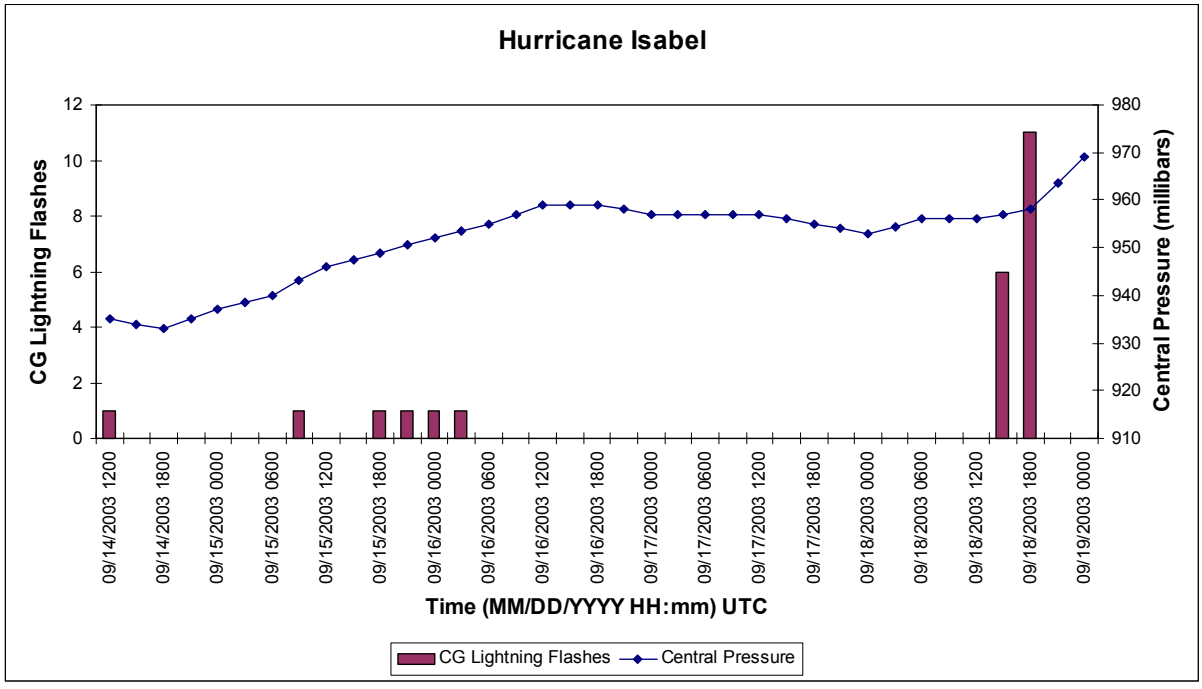

Figure 13. Three-hour CG lightning rates detected within 60 km of Hurricane Isabel's center superimposed on Isabel's central pressure. CG lightning rates are indicated by purple bars with values located on the left y-axis and central pressure is indicated by the blue line with values located on the right y-axis. (Fig. 5, Demetriades and Holle, 2005, with permission.)